Eur Biophys J (2013) 42:223–239
DOI 10.1007/s00249-012-0880-y

REVIEW

EBSA
Biophysics in Europe

Molecular dynamics of water in the neighborhood of aquaporins

Marcelo Ozu · H. Ariel Alvarez · Andrés N. McCarthy · J. Raúl Grigera · Osvaldo Chara

Received: 26 June 2012 / Revised: 4 December 2012 / Accepted: 11 December 2012 / Published online: 29 December 2012

Abstract Present knowledge obtained by molecular dynamics (MD) simulation studies regarding the dynamics of water, both in the vicinity of biological membranes and within the proteinaceous water channels, also known as aquaporins (AQPs), is reviewed. A brief general summary of the water models most extensively employed in MD simulations (SPC, SPC/E, TIP3P, TIP4P), indicating their most relevant pros and cons, is likewise provided. Structural considerations of water are also discussed, based on different order parameters, which can be extracted from MD simulations as well as from experiments. Secondly, the behaviour of water in the neighbourhood of membranes by means of molecular dynamics simulations is addressed. Consequently, the comparison with previous experimental evidence is pointed out. In living cells, water is transported across the plasma membrane through the lipid bilayer and the aforementioned AQPs, which motivates this review to focus mostly on MD simulation studies of water within AQPs. Relevant contributions explaining peculiar properties of these channels are discussed, such as selectivity and gating. Water models used in these studies are also summarised. Finally, based on the information presented here, further MD studies are encouraged.

Keywords Aquaporins · Water model · SPC/E · Water permeability · Molecular dynamics

Introduction

Living organisms are comprised by approximately 70 % water,[1] which is dynamically transported between each cell and its environment (including other cells), from one tissue to another, from one organ to another. At different scales, water transport takes place at accordingly different velocities, as well as at correspondingly adequate efficiencies, aspects that most likely occur as a result of the numerous conditions imposed by evolution. This transport is determined by the various biological structures with which water actually interacts. The physical peculiarities and particular geometry of the water molecule determine not only the interplay between these and the plasma membrane, but also between water molecules themselves.

In a small bacterial cell, the content of water is of the order of 10^{10} molecules[2] and is in general higher in eukaryotic cells. Such a huge amount of water molecules, together with the fact that there is not a sufficiently sensitive technique to detect only one water molecule, makes

Marcelo Ozu and H. Ariel Alvarez contributed equally to this work.

M. Ozu
Laboratorio de Biomembranas, Departamento de Ciencias Fisiológicas, Facultad de Medicina, Universidad de Buenos Aires, Buenos Aires, Argentina

H. A. Alvarez · A. N. McCarthy · J. R. Grigera · O. Chara
Institute of Physics of Liquids and Biological Systems (IFLYSIB), CONICET and University of La Plata (UNLP), La Plata, Argentina

O. Chara (✉)
Center for Information Services and High Performance Computing (ZIH), Dresden University of Technology, Nöthnitzer Straße 46, 01187 Dresden, Germany
e-mail: osvaldo.chara@tu-dresden.de

[1] In humans the total body water is a little bit lower than 70 %, being 61.8 % for males and 51.9 % for females, according to the classical study using deuterium oxide dilution (Schloerb et al. 1950).

[2] See, for instance: http://bionumbers.hms.harvard.edu/bionumber.aspx?s=y&id=100123&ver=0.

clear why experimental studies devoted to explain the behaviour of water in biological systems are essentially macroscopic. Therefore, although such experiments have provided vast information on these systems, it is clear that the molecular nature of water might be elusive from such a perspective. Fortunately, in silico approaches like Monte Carlo (MC) or molecular dynamics (MD) simulations have enabled the study of water at the nanoscopic level.

This review is focussed on the dynamics of water in the vicinity of membranes and aquaporins (AQPs), studied by molecular dynamics simulations.

The review is in three sections. The first section covers a brief introduction regarding the basics of the molecular dynamic simulations applied to water. This is followed by a section that addresses up-to-date studies on the behaviour of water in the neighbourhood of membranes.

In living cells, water is transported across the plasma membrane through proteins that work as water channels, also known as aquaporins. These proteins are widespread in nature, and much of their importance in physiological processes and diseases has been revealed in the last decade, resulting in the 2003 Nobel Prize for Peter Agre. Therefore, the last section of this article is devoted to an extensive review of the dynamics of water within AQPs. Additionally, we elaborate on the perspective of future studies, which could plausibly constitute a relevant contribution to the furthering of our knowledge on this matter.

Molecular dynamics of water, an introduction

Presently, there are several molecular dynamic models of water readily available for use in such simulations (Guillot 2002), ranging from planar to tetrahedral geometries, with rigid or flexible topologies, fixed or polarisable charges, with three, four, five or six single-point charges. We will here focus on analysing the properties of the four most popular rigid planar water models, i.e. SPC (Berendsen et al. 1981), SPC/E (Berendsen et al. 1987), TIP3P (Jorgensen et al. 1983) and TIP4P (Jorgensen et al. 1983; Jorgensen and Madura 1985).

The general characteristics of these four models are shown in Fig. 1. Their parameters are presented in Table 1, where $\boldsymbol{\sigma}$ and $\boldsymbol{\varepsilon}$ are, respectively, the Lennard-Jones collision diameter and the depth of the potential well (centred in the oxygen atom), and $\mathbf{L}$ is the distance between the centres of mass (COM) of the oxygen and hydrogen atoms. In all four models, the positive charge $\mathbf{q_H}$ is located over the hydrogen atoms. In the case of three site models, the negative charge $\mathbf{q_O}$ is placed over the oxygen. The HOH angle is called $\boldsymbol{\theta}°$. In the TIP4P model, $\mathbf{l}$ is the distance between the dummy position (D) where the negative charge is placed (near the oxygen along the bisector of $\boldsymbol{\theta}°$) and the oxygen centre of mass, and $\boldsymbol{\varphi}°$ is the angle between the OH segment and the OD segment (i.e. $\boldsymbol{\theta}° = 2\boldsymbol{\varphi}°$).

From a further look at the data presented in Table 1, it can be readily concluded that the SPC/E model is a re-parameterisation of the SPC model, taking into account the self-energy correction due to the effective molecular dipole moment of water in the liquid phase. Significantly, the SPC and SPC/E models show a wider $\boldsymbol{\theta}°$ angle than that of the actual molecule, with the electrical charge distribution being the only difference between these two models. On the other hand, the TIP4P model introduces a fourth point, a dummy site (without mass), where the negative charge is located. It also differs from the TIP3P in both charge distribution and Lennard-Jones parameters. Interestingly, such differences between these water models induce distinctive differences in the values of physical properties shown by each. Namely, the SPC/E model presents a better density and diffusion constant than the SPC model. All of these models show poor agreement as regards the melting point of water (giving melting points of 190, 215, 146 and 232 K respectively) (Vega et al. 2005).

As marked in bold in Table 2, the SPC/E model presents better values for the density, dipole moment, self-diffusion constant, potential energy per mole and dielectric constant, while the TIP4P model provides better values for the density maximum, temperature and expansion coefficient. From these observations it may be concluded that, when studying a particular physical property, the use of a single model might be the best option. For instance, if the study were based on the temperature at which density achieves its maximum, then the TIP4P model should probably be chosen. However, it is clear that the SPC/E model presents a better average performance as regards the physical properties mentioned above at a lower computational cost.

Regardless of the aforementioned modelling perspective, the actual physical properties of water, as obtained from the experiment, may be clearly distinguished from those observed for non-associated liquids and are notoriously susceptible to modification by changes in temperature and pressure conditions, as has been extensively shown through various experimental approaches (Castner et al. 1995; Danninger and Zundel 1981; Gale et al. 1999; Laenen et al. 1998; Modig et al. 2003; Montrose et al. 1974; Narten et al. 1967; Nienhuys et al. 1999; Soper et al. 1997; Woutersen et al. 1997; Yeixeira et al. 1991). Such results show that the so-called ‘anomalies’ of water are gradually lost as temperature and pressure increase, moving towards a regime similar to that of a simple liquid. These peculiar physical properties of water have long been recognised, widely associating the existence of such particularities with the unique structure of water. In order to quantify the referred structure changes, many order parameters have been proposed, as is briefly summarised below.

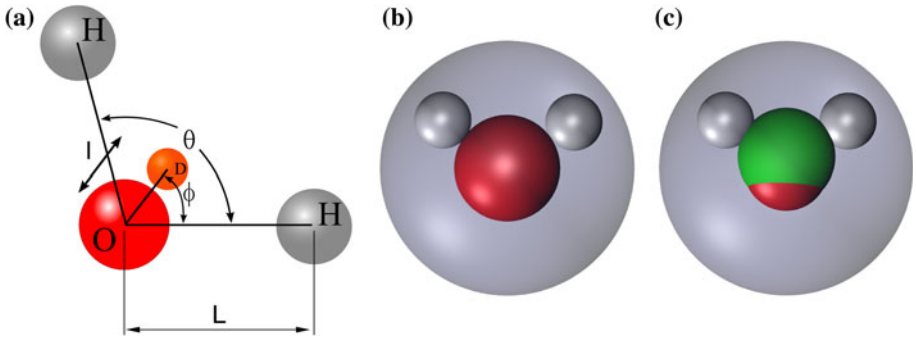

Fig. 1 Schematic representation of some of the most popular simple planar molecular models of water. **a** Parameters of the models (the fourth point, named D, is the position of the dummy atom, only present in TIP4P). **b** Three site models (i.e. SPC, TIP3P and SPC/E). **c** Four-point model (TIP4P). In Fig. 1a, b, the big sphere represents the van der Waals potential

Table 1 Parameters of the described models

Model	L-J parameters		L (10^{-10} m)	l (10^{-10} m)	q_H (e^-)	q_O (e^-)	θ°	ϕ°
	σ (10^{-10} m)	ε (kJ mol^{-1})						
SPC	3.166	0.650	1.0000	–	+0.410	−0.8200	109.47	–
SPC/E	3.166	0.650	1.0000	–	+0.4238	−0.8476	109.47	–
TIP3P	3.15061	0.6364	0.9572	–	+0.4170	−0.8340	104.52	–
TIP4P	3.15365	0.6480	0.9572	0.15	+0.5200	−1.0400	104.52	52.26

σ: Lennard-Jones collision diameter; ε: depth of the potential well; L: distance between the centres of mass (COM) of the oxygen and hydrogen atoms. qH: positive charge; qO: negative charge; is called θ°: HOH angle; φ°: angle between the OH segment and the OD segment (i.e. $\theta° = 2\varphi°$); l: distance between the dummy position (D in Fig. 1) where the negative charge is placed (near the oxygen along the bisector of θ°) and the oxygen centre of mass

Table 2 Calculated physical properties of the presented water models and their respective experimental values (all the data are at 298 K and 1 atm, except * at 300 K and # at 293 K)

Model	SPC	SPC/E	TIP3P	TIP4P	Experimental
Density, ρ (kg/m^3)	970*[a]	**998*[a]**	1002[i]	1001[i]	997[i]
Dipole moment, μ (D)	2.27[b]	**2.39[b]**	2.35[b]	2.18[b]	2.95[l]
Dielectric constant, ε (adimensional)	65[c]	**68[c]**	97[c]	53#[j]	78.39[m]
				29*[k]	
Self-diffusion constant, D (10^{-5} cm^2/s)	3.85[d]	**2.49[d]**	5.19[d]	3.31[d]	2.30[n]
Average configurational energy, U (kJ mol^{-1})	−37.7[a]	**−41.4[a]**	−41.1[i]	−42.1[i]	−41.5[o]
Density maximum, T_{TMD} (K)	228[e]	235[g]	182[e]	**253[e]**	277.13[p]
Expansion coefficient, α_p (10^{-4} $°C^{-1}$)	7.3*[f]	5.14[h]	9.2[i]	**4.4[i]**	2.53[q]

[a] Berendsen et al. (1987), [b] van der Spoel et al. (1998), [c] Höchtl et al. (1998), [d] Mahoney and Jorgensen (2001), [e] Vega and Abascal (2005), [f] Yu and van Gunsteren (2004), [g] Báez and Clancy (1994), [h] Wu et al. (2006), [i] Mahoney and Jorgensen (2000), [j] Neumann (1986), [k] Strauch and Cummings (1989), [l] Gubskaya and Kusalik (2002), [m] Vidulich et al. (1967), [n] Krynicki et al. (1978), [o] Postma (1985), [p] Franks (2000), [q] Kell (1975)

Physical properties that show most similar values to experimental determinations are indicated in bold

Truskett and co-workers proposed the translational order parameter *t*, which quantifies the tendency of pairs of molecules to adopt preferential separations, being negligible for an ideal gas, and having large values for a crystal (Truskett et al. 2000). *t* gives a general idea of the structure. However, in order to elucidate the nature of the structure, other parameters are necessary.

Tetrahedrality was tested by both the *Q3* (proposed by Steinhardt et al. 1983) and *T* (proposed by Kiselev et al. 1993; and Naberukhin et al. 1991) parameters. Nevertheless, as has been discussed elsewhere (Chau and Hardwick 1998), *Q3* shows two drawbacks. First of all, the tetrahedral value for *Q3* can be obtained only when the configuration is of a certain pyramidal shape, and second, the tetrahedral configuration value is not a limiting value, which in some cases could result in a mean value close to tetrahedrality, whilst the actual configurations are not tetrahedral at all. On the other hand, the *T* parameter involves

two complications: since each evaluation implies the calculation of ten distances, it is highly expensive computationally; additionally, it is not easy to connect its value to the configurational geometry. To solve the aforementioned drawbacks, Chau and Hardwick (1998) proposed the parameter *S*. This parameter is composed of two parts, *Sg* and *Sk*. *Sg* is used to test for the existence of tetrahedral angles, and its value can be mapped to the geometry of the configuration. *Sk* is the variance in the radial distance from the central vertex to the other four vertices. From the parameter *S* we can know how distorted the polyhedron is, and in what way. A weakness of *S* is that it is not easy to connect the value of *Sk* to the configurational geometry.

Errington and Debenedetti (2001) used an enhanced version of the parameter *S* (they used a rescaled version of *S*, which they called *q*) in order to study the changes in structure of the SPC/E water model under various temperature and pressure conditions. The authors showed a bimodal distribution for this parameter, concluding that each water molecule and its four nearest neighbours transiently present an arrangement (Sciortino et al. 1990, 1991; Shiratani and Sasai 1998), which can be described as either following an 'ice-like' structure or not.

To calculate all the aforementioned parameters, information on the position of every oxygen atom in water bulk is necessary. This condition restricts the use of the above parameters to computational studies only. Moreover, all the previously discussed parameters that evaluate tetrahedrality are explicitly restricted to the evaluation of the first coordination sphere.

To overcome the mentioned drawbacks a new parameter was recently proposed (Chara et al. 2011). This parameter, P_r, comes from the idea that water in liquid state can be regarded as a combination of closely interwoven low- and high-density structures, as originally proposed in the seminal work of Bernal and Fowler (1933). These structures correspond to an open (tetrahedral) and a closed (hexagonal) conformation, respectively. P_r is able to evaluate structure beyond the first coordination sphere. Additionally, its calculation requires only the information provided by a probability density function for the position of water oxygen atoms, i.e. the radial distribution function $g(r)$. Such information may be readily obtained by both computational and experimental studies. The parameter P_r is defined as:

$$P_r = \frac{C_t - C_h}{C_t + C_h} \tag{1}$$

where C_t and C_h are the tetrahedral and hexagonal contributions, which can be estimated from the $g(r)$.

Using molecular dynamics simulations under various temperature and pressure conditions, it was demonstrated that, for SPC/E, P_r follows a monotonically decreasing behaviour with pressure. This result may be interpreted adducing that pressure is 'disturbing' the hydrogen bond network linking water molecules together, forcing some of these that formerly belonged to the tetrahedral set into a hexagonal conformation. Interestingly, following this interpretation, a pressure in which no prevalence between both structural contributions clearly appears: the crossover point.

Hence, this parameter is able to establish the point in which the change in predominance between the tetrahedral and hexagonal structural contributions occurs in reference to pressure and temperature changes. Consequently, through the use of this parameter, it was possible to demonstrate that the increase in both pressure and temperature induces an increase in the hexagonal structural contribution of water to the detriment of the tetrahedral one (Chara et al. 2011).

Pressure and temperature change can induce notable modifications in water properties, which evince the dynamic and structural alterations through the adaptation of the hydrogen bond network. These alterations can be readily monitored using a variety of previously reviewed order parameters, given that the mentioned limitations each parameter presents are readily regarded.

The previous order parameters proved effective not only for water in 3D–bulk–state studies, but also under different confinement degrees from 2D water near a membrane (Deshmukh and Sankaranarayanan 2012) and hydration water surrounding a macromolecule such as lysozime to the DNA environment (Kumar et al. 2006)—or 1D confinement—within a nanopore (Weng et al. 2008; Lerbret et al. 2011). Interestingly, in biological systems, water molecules typically interact with surfaces or interfaces, which in turn confine them. In the next section we review various studies on how such confinement conditions ultimately alter the water structure.

Molecular dynamics of water in the presence of membranes

In the previous section we addressed the study of non-confined water, i.e. water in bulk conditions. From this previous section and the articles cited therein, it is clear that water molecules participate in structures that become stabilised by a great diversity of hydrogen bond networks (Jeffrey and Saenger 1994; Pimentel and McClellan 1960).

Water forms many polymorphs, characterised by structural and kinetic features, which are receptive to the influence of several factors. The confinement of water can produce alteration in its behaviour, mainly through the disruption of such hydrogen bond networks. Also, it is expected that the eventual hydrophobicity of the

confinement surface may modify water behaviour in its neighbourhood.

The effect of hydrophobic walls on the properties of neighbouring water has been largely studied, both from experimental and computational points of view.

Since the early 1980s, much experimental evidence has established that long range effects exist between two hydrophobic walls separated by water (Boehnke et al. 1999; Craig et al. 1999; Ederth and Liedberg 2000; Israelachvili 1992; Israelachvili and McGuiggan 1988; Israelachvili and Pashley 1982; Tsao et al. 1993), as well as by other solvents, which manifest a solvophobic effect, such as ethylene glycol (Boehnke et al. 1999; Parker and Claesson 1994; Zhu and Robinson 1991). However, these long-range experimental results could not be corroborated by most of the related computational studies available in the literature (Gentilcore et al. 2010; Gordillo et al. 2005; Grigera et al. 1996; Lee et al. 1984; Lee and Rossky 1994; Spohr 1997; Striolo et al. 2003, 2004), thus only reporting the manifestation of short-range effects through computational studies.

A natural question arises as to why such studies were unable to reproduce these experimental observations. The first part of the answer could arise from analysing the common factor between them. In the first place, all computational studies report the use of distances smaller than 1.7 nm between the hydrophobic wall and the proposed water bulk (Lee and Rossky 1994). Moreover, and most important, all studies have evaluated the degree of order in the water phase using either density or average hydrogen bond number, or both. Nevertheless, these two parameters might be incapable of accounting for certain subtle, yet substantial, structural variations within the vicinity of a hydrophobic surface.

In order to overcome the two aforementioned pitfalls, the behaviour of water molecules in the neighbourhood of hydrophobic and hydrophilic membranes at different temperatures was later studied (Chara et al. 2009), both enhancing the dimensions of the system under study and designing more subtle structural quantifiers for the evaluation of the eventual structural changes of water. In this work, the distances between membranes were approximately 170 A; in accordance with the mentioned references, no influence was evidenced through density calculations as a function of the perpendicular distance from the membranes.

Self-diffusion coefficient and energy activation for water showed subtle alterations due to the presence of membranes. However, the hydrogen bond distribution showed that the probability of one water molecule interacting with four neighbouring water molecules is higher close to a hydrophobic membrane, relative to bulk conditions. Such an observation is valid even at distances as great as 60 Å from the hydrophobic membrane (Fig. 2).

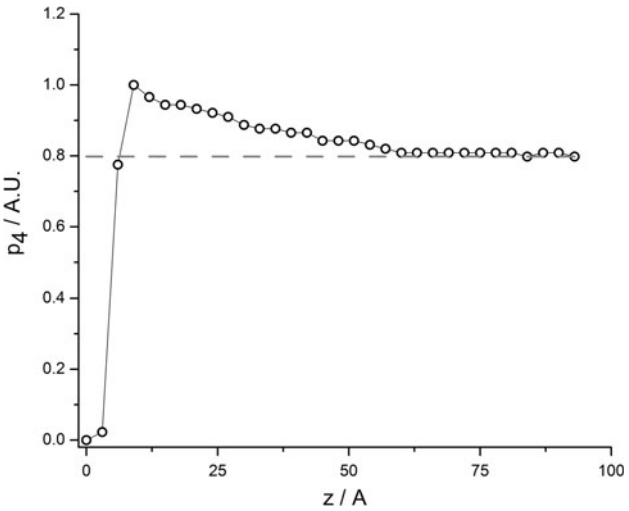

Fig. 2 Probability of one water molecule to interact with four water molecules in its neighbourhood (p_4, continuous curve) calculated all along the length perpendicular to a hydrophobic membrane (located at $z = 0$ A). p_4 reaches a convergence value (*dotted curve*) within a distance of 60 A from the membrane. Simulation involved SPC/E at a pressure and temperature of 1 bar and 300 K, respectively. Reprinted from Chara et al. (2009), with permission from Elsevier

Thus, it appears that a hydrophobic membrane induces an ordered or 'ice-like' phase in water. This structural enhancement involves roughly 18–24 water hydration layers, depending on temperature conditions. Reasonably, such structural enhancement is what the hydrophobic effect is all about, i.e. water molecules become "disordered" when moving from an "enhanced order state" within the neighbourhood of a hydrophobic membrane to a "base order state" within the water bulk. Interestingly, the range of membrane influence on the surrounding water molecules is of the order of that of a plasma membrane. Hence, it could be speculated that the short-lived exposition of hydrophobic regions of proteins or lipids in a plasma membrane could readily induce transient alterations in the structure of water within distances of the same order as that of the plasma membrane. These alterations are expected to be of great importance in confined systems such as natural nanopores, i.e. the water channels or aquaporins.

Molecular dynamics of water within aquaporins

This section is about water confined in pores of nanometre dimensions, an issue that made possible the understanding of the behaviour of water molecules inside natural water channels, i.e. aquaporins (AQPs).

The history of the water channel hypothesis was supported by experimental evidence provided by physiologists, although it took several decades to confirm the actual

existence of water channel proteins. Meanwhile, several studies supported interesting theories regarding the behaviour of water inside channels and the nature of the osmotic movement. However, these hypotheses have not yet been proved experimentally because of technical limitations. Fortunately, in silico experiments have allowed the confirmation of some of these, mainly by means of molecular dynamics simulations. In this section we review the main issues concerning the nature of water transport through channels of nanometre dimensions, as arises from computational studies based on these conventional water models. Such studies have led to deepening and strengthening most of the ideas that experimental researchers have discussed and elaborated on for many years, often bordering on arguments of philosophical dimensions.

Recognition of aquaporins

The existence of facilitated pathways for the passage of water through biological membranes was a hypothesis supported by experimental physiologists and biophysicists. Although some evidence indicated that water channels had to be proteins, it was not until 1992 that experimentalists accepted the existence of water channels of a protein nature (for a detailed review, see Parisi et al. 2007). At almost the same time, P. Agre published the first protein clone with clear water channel characteristics (Preston et al. 1992). This protein, first called CHIP28, was then renamed AQP1, i.e. aquaporin 1, as it was the first to be discovered. To date, 13 mammalian aquaporins have been discovered. All of them are expressed in humans, and their malfunction is related to several diseases (Table 3). For example, several recent studies on aquaporins have been centred on AQP4. This channel protein is expressed in the brain and its function has a relevant role in the development of neuromyelitis optica (NMO), which is a rare demyelinating disease that selectively affects the optic nerve and the spinal cord in humans (for a review on this subject, see Graber et al. 2008).

To date, the crystal structure of aquaporins from ten different subfamilies has been resolved: AQP1 (Murata et al. 2000; Ren et al. 2000; Sui et al. 2001), AQP0 (Murata et al. 2000; Sui et al. 2001), GlpF (Fu et al. 2000; Tajkhorshid et al. 2002), AQPZ (Jiang et al. 2006; Savage et al. 2003), SoPIP2;1 (Gonen et al. 2004; Törnroth-Horsefield et al. 2006), AQPM (Lee et al. 2005), PfAQP (Newby et al. 2008), AQP5 (Horsefield et al. 2008), AQP4 (Ho et al. 2009; Tani et al. 2009) and Aqy1 (Fischer et al. 2009). Additionally, the molecular forces that interact between adjacent transmembrane segments in AQP1 have been measured using atomic force microscopy (Möller et al. 2003).

All the members of the AQP family are small, very hydrophobic, intrinsic membrane proteins, which are present in the membrane as tetramers. Nevertheless, the channel for water permeability does not reside in the centre of the tetramer (as it does for ion channels). Instead, each monomer constitutes a channel (Verkman and Mitra 2000). Predicted sizes for the monomer of the mammalian AQPs range from 27 to 31 kDa (Verkman and Mitra 2000). The sequence alignment of the AQPs monomers shows several highly conserved motifs, among which two repeating Asn-Pro-Ala's (NPA) (Jung et al. 1994) are highlighted. These are known as the signature sequence motifs of these proteins. The conformation of each monomer in the membrane shows six membrane-spanning α-helices and two long loops, one cytosolic (loop B) and the other extracellular (loop E). Both the N and C termini of the proteins are intracellular. One NPA motif is located in loop B and the other in loop E. These loops deepen into the membrane constituting a seventh transmembrane pseudo helix, opposing the two NPA motifs near the centre of the channel. The AQPs also share another highly conserved sequence, the aromatic/arginine (ar/R) region, which exits at the extracellular side of the channel and constitutes the selectivity filter of the protein (Fig. 3).

Structural studies have provided a relevant insight regarding the determining requirements that enable homotetramer formation, the quaternary structure that actually enables water transport activity in animal AQPs (Smith and Agre 1991; Walz et al. 1994; Mathai and Agre 1999). In plants, this heterotetramer organisation of AQPs apparently constitutes a form of regulation for monomer transport rates (Bellati et al. 2010; Fetter et al. 2004). However, in AQP4, the existence of a heterotetramer formed by two splice variants (M1 and M23) of protein has been reported (Neely et al. 1999).

Mercurial sulfhydryl reagents such as $HgCl_2$ inhibit water channel-mediated water permeability. In AQP1, the residue Cys^{189} has been shown to be the site of mercurial binding and water transport inhibition (Preston et al. 1993). This inhibition mechanism was elucidated at a molecular level by MD simulations with the AMBER 8 program package (Hirano et al. 2010). According to alignment comparison with AQP1, other AQPs have cysteine residues at identical locations in their amino acid sequences. However, it was demonstrated that not all AQPs are inhibited by $HgCl_2$. The characteristic case is AQP6, whose water permeability is increased in the presence of this mercurial agent (Yasui et al. 1999).

In another aspect, atomistic MD simulation can help to clarify a controversial issue about the selectivity mechanisms of AQPs: the passage of CO_2 and other gases through these proteins (Fang et al. 2002; Nakhoul et al. 1998; Verkman 2002). While some experimental researchers affirm that CO_2 passes through AQP1 (Cooper et al. 2002; Prasad et al. 1998), MD simulations using the TIP4P water model with GROMACS simulation software

Table 3 Mammalian AQPs

	Transport	Organ expression	Related disease[a]
AQP0	Water	**Eye**	Cataract
AQP1	Water	Brain, eye, heart, lung, GI tract, salivary gland, liver, ovary, muscle, erythrocyte, spleen	Polyuria, mild urine concentration
AQP2	Water	**Kidney**	Severe polyuria, diabetes insipidus
AQP3 (GLP)	Water, urea, glycerol	**Kidney**, heart, ovary, eye, salivary gland, GI tract, brain, erythrocyte	Urinary concentrating defect, delayed wound healing, reduced skin hydration, reduced elasticity
AQP4	Water	**Brain**, kidney, salivary gland, heart, GI tract, muscle	Mild urine-concentrating defect, reduced injury-induced brain oedema, hearing defects
AQP5	Water	**Salivary gland**, lung, GI tract, ovary, eye	Impaired salivary secretion, impaired stimulated sweat secretion, impaired secretion in airway submucosal glands
AQP6	Anions, water	**Brain**, kidney	
AQP7 (GLP)	Water, urea, glycerol, arsenite	**Testis**, heart, kidney, ovary	Decreased glycerol metabolism, increased body fat and body weight
AQP8	Water, urea, NH_3	**Testis**, **liver**, pancreas, ovary, lung	Mild hypertriglyceridemia
AQP9 (GLP)	Water, urea, glycerol, arsenite	Liver, spleen, testis, ovary, leukocyte	
AQP10 (GLP)	Water, urea, glycerol	**GI tract**	
AQP11	Unknown	**Testis**, heart, kidney, ovary, muscle, GI tract, leukocytes, liver, brain	Polycystic kidney disease
AQP12	Unnown	**Pancreas**	

Those members with aquaglyceroporin activity are indicated as GLP between brackets. The organ with the most important expression is indicated in bold

[a] Related diseases observed in mouse. GI tract refers to gastrointestinal tract. For a review of aquaporins in mammals, see Ishibashi et al. (2008)

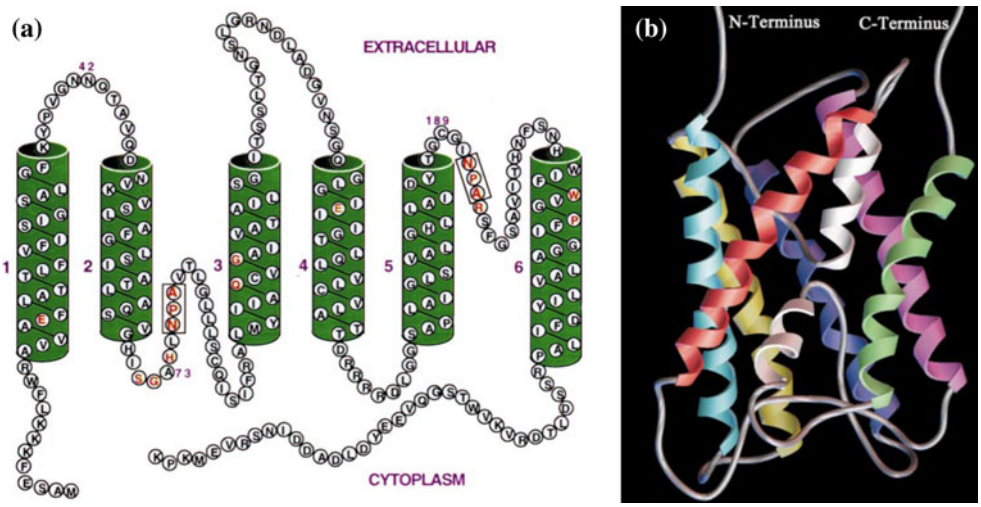

Fig. 3 Schematic representation of AQP1. **a** Scheme of the protein sequence, indicating the six transmembrane segments, the two NPA motifs and clue residues. **b** Scheme of the special conformation of one monomer. Reprinted from Ren et al. (2000), with permission from Elsevier

indicate that this would be the case in biological lipid bilayers with a low intrinsic CO_2 permeability (Hub and de Groot 2006). In addition, it has been shown, using the same water model, that water channel interactions, not solute channel interactions, are the key determinants underlying the selectivity mechanism of AQPs. Hence, the hydrophobic effect, together with steric restraints, determines the selectivity of AQPs (Hub and de Groot 2008).

The case of AQP0 is particular because this aquaporin shows p_f values approximately 100-fold lower than AQP1 (Zampighi et al. 1995), conferring only a four-to-five-fold increase in water permeability over the intrinsic

permeability of lipid bilayers. Since these earlier physiological studies, AQP0 has been thought to have another physiological function (Mulders et al. 1995). Based on the structural determination and MD simulation studies, it was proposed that AQP0 could be an "adhennel", a term that describes a membrane protein that functions both as a cell adhesion molecule and a membrane channel (Engel et al. 2008; Han et al. 2006). Using the TIP3P model (CHAMM27 force field), it was recently shown that the reason why AQP0 has low p_f values is that the water chain inside the pore is disrupted in the region of residue Tyr23 (Qiu et al. 2010).

The study of water passing through narrow channels

Studying the behaviour of water confined in nanometer-dimension pores

While AQPs were discovered by experimental researchers, MD simulations were performed in order to understand the structure of water molecules inside a channel by very well known to experimentalists: the gramicidin A channel. Thus, using the GROMOS package and the SPC water model, it was first shown that water molecules act as a collective chain inside the gramicidin A channel and that all the water molecules are oriented with their dipole moments pointing parallel to the pore axis (Chiu et al. 1989). Next, through the addition of various water layers at both ends of the channel, it was observed that individual water molecules confined in the channel executed higher frequency motions than bulk water and that the mobility of the water chain became reduced with the rigidity of the channel (Chiu et al. 1991). This result was obtained with the SPC water model, which presents a self-diffusion coefficient in bulk $\sim$1.67 times larger than the experimental value (Table 2). In a further step, the complexity of the system was increased in order to create a system in which the water-filled channel is set into a lipid bilayer (Chiu et al. 1999). In this case, the SPC/E water model was used, which presents almost exactly the same self-diffusion coefficient as determined experimentally for bulk water (Table 2). The results indicated that the mobility of water inside the gramicidin channel was similar to that of bulk self-diffusion coefficient. These first MD studies of water behaviour within protein channels may be regarded as reasonable approximations to be readily furthered once the crystallographic structure of AQPs has been resolved (Murata et al. 2000; Ren et al. 2000).

Almost in parallel, numerous MD simulations focussed on water behaviour within nanopores.[3] Lynden-Bell and Rasaiah (1996) used the SPC/E water model to simulate the motion of ions and water inside smooth infinite cylindrical pores. Their results indicated that water forms a solvation shell inside the channel. Smaller ions (with a 3-Å radius) lie preferentially in the centre of the pore, while larger ions penetrate the solvation shell. These results indicated that water density is non-uniform inside the channel. Concurrently, Monte Carlo simulations using the PSPC water model (a variation of SPC) demonstrated that large external electric fields (up to 3×10^9 V m^{-1}) pulled water molecules to the walls inside the pore and that changes in pore geometry alter water density and hence its structure inside the pore (Green and Lu 1997). Subsequently, the standard rigid five-site ST2 water model was used to test the self-diffusion capacity of water and ions inside hydrophobic and hydrophilic pores of different sizes (Allen et al. 1999). The ST2 water model has a bulk water self-diffusion value very close to the actual experimental value, only improved by the SPC/E water model. The obtained results showed that in hydrophobic pores water structure and self-diffusion exhibit a dramatic dependence in pore size because of the packing of the hydrogen bonded networks. Lately, studies using the SPC water model succeeded in showing that purely hydrophobic pores suffer transitions between an open and a closed state (Beckstein et al. 2001). The closed state occurs when there is no water in the pore cavity and the open state when the water density inside the pore cavity is approximately that of bulk water. Curiously, this shift occurs once a critical pore radius has been exceeded (Beckstein et al. 2001). In addition, the density of water inside the pore depends on the fluid-wall interactions and is smaller than the bulk liquid density, but when the radius and/or hydrophilicity of the pore increase, the fluid density inside the pore approaches that of bulk liquid (Giaya and Thompson 2002). These results indicate that water inside small hydrophobic material pores seems to be in a vapour state and that this depends on the geometrical characteristics of the pore. The kinetic analysis of this transition was studied in long simulations (460 ns) using the SPC model. The results indicated that water flow through the pore occurs in bursts because of transitions inside the pore between a vapour state and a liquid state (Beckstein and Samson 2003). These observations supported the idea that water, inside pores of nanometre-dimensions, behaves as a gas (Zhou et al. 2004).

Later on, new evidences from MD simulations in nanotubes supported the idea that water inside a pore is in a vapour-like state and that the penetration of water inside pores is modulated by the polarity and the structure of the cavity (Beckstein and Samson 2004; Vaistheeswaran et al. 2004a, b), as well as by electric fields that may affect the orientation of water molecules inside the channel

[3] One of the first MD simulations of water diffusion inside nanopores was done by D.G. Levitt (1973), using pores that were 11 Å long and 3.2 Å in radius and hard smooth spheres to simulate water molecules.

(Vaistheeswaran et al. 2004a, b). Despite the properties of the nanotube, the structure of bulk water outside the pore (studied with the TIP3P model) affects the permeation of water across a nanochannel (Gong et al. 2008). Thus, the cumulative results obtained from MD simulations in carbon nanopores have provided a wider picture of what may be happening inside AQPs.

Theoretical bases to study the transport properties of aquaporins by molecular dynamics

The study by MD of water passing through narrow pores posed a theoretical challenge. The simplest model was to think of water as filling pores in a single file fashion. Then, one water translocation event from one side of the channel to the other should occur when one water molecule enters the pore at one end, and simultaneously another water molecule leaves the channel at the other end. This simple model implies that the pore is always filled with water molecules and that water molecules move stochastically and concertedly along the axis of the pore. This is known as the continuous-time random walk (CTRW) model (Berezhkovskii and Hummer 2002), which was developed to explain the transport of water filling a channel in a single-file arrangement, which was previously simulated using the TIP3P water model (Hummer et al. 2001). However, the study of AQPs requires the ability to characterise their function properties. Hence, the diffusional (p_d) and osmotic (p_f) permeability coefficients are clear targets to be quantified. The strategy to determine p_d is simple, because this coefficient describes water movement by thermal fluctuations. Therefore, p_d can be determined from equilibrium MD simulations. Experimentally, p_d can be determined by the flux of labelled water molecules, e.g. by isotopic replacement (Finkelstein 1987). Using the CTRW model, p_d can be determined by

$$p_d = \frac{v_w \cdot k_0}{N+1} \tag{2}$$

where v_w is the average volume of a single water molecule, k_0 is the hopping rate of water molecules that enter or leave the channel, and N is the number of water molecules that occupy all the AQP channel in single file (Zhu et al. 2004a). The case of p_f is different because this coefficient accounts for translocation events induced by osmotic differences, thus implying non-equilibrium conditions. The challenge in this case is to simulate osmotic pressures. The strategy is based on the fact that the osmotic flux depends on the difference of chemical potentials (Δu) between both reservoirs. Therefore, p_f can be calculated from

$$p_f = v_w \cdot k_0 \tag{3}$$

where k_0 relates the net water flux with Δu. Since

$$\Delta u = v_w \cdot \Delta P \tag{4}$$

(Finkelstein 1987), osmotic differences can be simulated inducing hydrostatic pressures (ΔP) (Zhu et al. 2004a). From Eqs. (2) and (3), the following expression can be straightforwardly obtained.

$$\frac{p_f}{p_d} = N + 1 \tag{5}$$

This expression was applied to molecular dynamic simulations of water (modelled with TIP3P) within AQP1 and it is in agreement with calculations based on experimental data (Parisi and Bourguet 1983).

Although inducing hydrostatic pressure differences is a practical strategy, very large ΔPs are needed to simulate induced fluxes by MD. This has the inconvenience that simulated conditions are far from experimental conditions, generating uncertainty regarding the fact that the results thus obtained may not correctly represent the normal kinetics of water within the channel. However, when assuming a collective diffusion model, the water movement in a stationary state can be analysed as diffusional events in equilibrium (Zhu et al. 2004b). According to this model, which was also developed based on MD simulations using the TIP3P model for water, the slope of the mean square displacement (MSD or $\langle n^2(t) \rangle$), plotted against the time spent by water molecules inside the channel, represents p_f. Moreover, this model accounts for single file situations as well as collective water movements through wider pores where water molecules do not span the channel in single file. These and other determinations of p_d and p_f of AQPs, using the TIP3P model for water (Mamonov et al. 2007), are in close agreement with experimental determinations.

It is notable that although previous MD nanopore-water simulations were performed using various rigid water models, the studies that established the theoretical basis to elucidate the p_d and p_f coefficients of AQPs were developed using the TIP3P water model.

Later on, the TIP4P water model was used in atomistic MD simulations using gramicidin channels of different lengths to demonstrate that the osmotic water permeability is independent of the pore length (Portella et al. 2007). This result was at variance with the assumption that this relationship should be linear, which had largely been accepted until that time (Finkelstein and Rosenberg 1979). In other studies, the same group used the same water model (TIP4P) to show that water molecules permeating through narrow non-single-file channels behave like independent single-file columns and present a general relationship between osmotic and diffusive water permeability coefficients (p_f and p_d, respectively), which shows that, in the single-file regime, the relation between these two coefficients

accounts for the time-averaged pore occupancy (Portella and de Groot 2009).

Diving into the aquaporin channel: the mechanism of proton exclusion

The first elucidated structure was that of AQP1, by electron microscopy at 3.8-Å resolution (Murata et al. 2000; Ren et al. 2000), which was later improved by x-ray crystallography at 2.2-Å resolution (Sui et al. 2001). With the structure elucidated, MD simulation studies were profusely undertaken. In 2001, de Groot and Grübmuller, at variance with other groups that used the TIP3P water model, used the SPC water model to report the first evidence showing that water molecules pass through the pore of AQP1 in single file (de Groot and Grubmüller 2001). By means of 'real-time' MD simulations, this pioneering work confirmed the hypothesis posed almost 20 years earlier (see the review by Parisi et al. 2007). Additionally, through experiments these studies also showed a behaviour that was unimaginable: that water molecules enter the pore with their dipole in one orientation and leave the pore at the other side with their dipole inverted 180° (Fig. 4). The characteristic of this behaviour is that there is a critical site in the pore where a single water molecule interrupts the water chain, with molecules located at both sides, albeit interacting only with the channel. This site is the fingerprint sequence of AQPs, the NPA motifs.

Although it was well known that protons are incapable of being translocated through AQP1 (Zeidel et al. 1992), the mechanism underlying this observation was unknown. With the first MD simulations performed on AQP1, this mechanism was postulated as related to the inversion of the water dipole inside the pore (de Groot and Grubmüller 2001). The same water molecule behaviour was observed when studying the glycerol uptake facilitator GlpF channel from *Escherichia coli*, although in this case the TIP3P water model was used. The explanation for the impaired proton translocation through aquaporins was that the proton wire is interrupted because of the dipole inversion of this water molecule (Tajkhorshid et al. 2002). However, a new MD report showed that the water/proton selectivity in AQP1 is controlled by the change in the solvation-free energy upon moving the charged proton from the water bulk to the channel (Burykin and Warshel 2003). Almost simultaneously, two other groups arrived at this same conclusion. Bert de Groot and co-workers used multiple non-equilibrium molecular dynamics simulations in AQP1, again using the SPC water model, in order to demonstrate that what prevents the proton passage through the channel is an electrostatic barrier of 25–30 kJ mol^{-1}, centred around the fingerprint Asn-Pro-Ala (NPA) motif, and not the interruption of the hydrogen-bonded water chain (de Groot et al. 2003). In addition, the study of electrostatic interactions between water molecules (TIP3P model) and the *Escherichia coli* glycerol uptake facilitator (GlpF) channel showed that the electrostatic field through the protein channel both explains the bipolar orientation of water in single file and blocks proton transport (Jensen et al. 2003). Again, according to MD simulations using the TIP3P model, the electrostatic barrier apparently arises from the distribution of charged and polar groups of the protein (Chakrabarti et al. 2004), but the NPA motif does not seem to be responsible for the solvation barrier (Burykin and Warshel 2004).

Although the final conclusion presented as a result of the present studies is that proton translocation through AQPs is prevented by electrostatic barriers, some differences were observed using different water models. As mentioned by Jensen and coworkers (2003), the TIP3P model (CHARMM27 parameter set) showed very little disruption of the water-hydrogen-bonded network at the SF region, in clear contrast with the observation made by de Groot and Grubmüller (2001) using the SPC model (GROMACS force field).

Motivated by the MD predictions summarised above, a voltage clamp study confirmed the impediment of GlpF to transport protons, the limit being the H^+/H_20 ratio 2.10^{-9} (Saparov et al. 2005). On the other hand, by introducing single- and double-point mutations in AQP1, it was demonstrated that AQP1 mutants can transport protons (among other solutes) and that the diameter at the ar/R region determines the solute permeability (Beitz et al. 2006), and furthermore confirmed the prediction made by MD simulations with the AMBER-99 force field and the TIP3P water model that protons do not pass through AQP1 by a Grotthuss mechanism, i.e. by means of a proton wire (Li et al. 2011).

Exploring the pore of the protein: gating mechanisms

Perhaps the most interesting features of channels are both their gating properties and the mechanisms underlying their gating ability. In the case of proteins belonging to the aquaporin family, gating mechanisms were clearly described experimentally in members of the vegetable kingdom. Possibly, this is due to the fact that some of the members are regulated by Ca^{2+} ions, phosphorylation, pressure or even light (for a review on these issues, see Törnroth-Horsefield et al. 2010). The spinach aquaporin SoPIP2:1 switches between open and closed states depending on the conformation of the cytoplasmic D-loop (Törnroth-Horsefield et al. 2006). MD simulations using the TIP3P water model on SoPIP2:1 indicate that residues Arg^{190}, Asp^{191} and Ser^{36} would be important in determining the open and the closed states of the channel

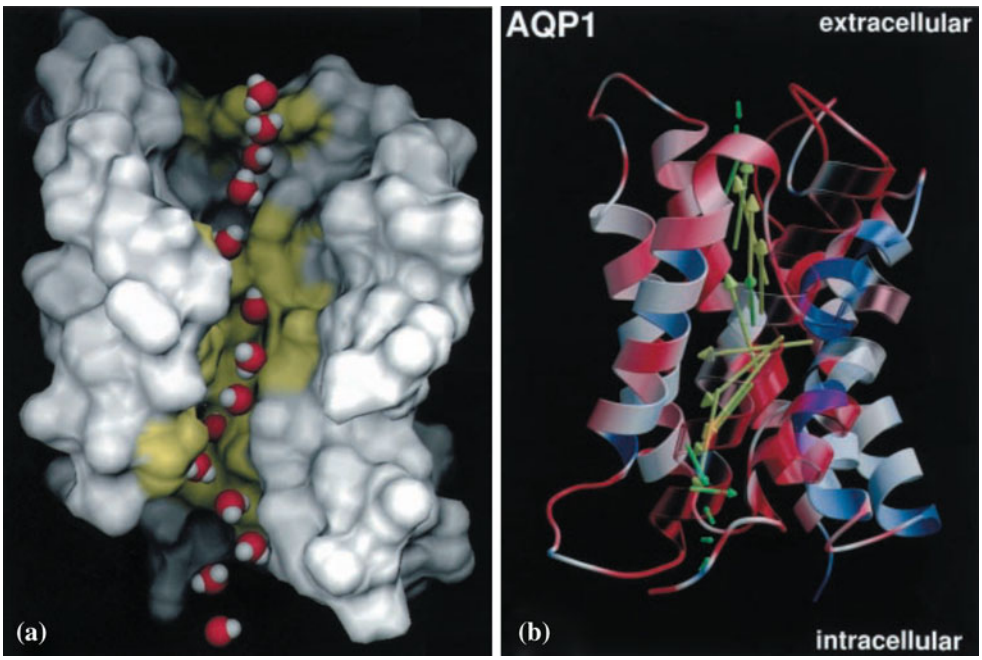

Fig. 4 Schematic representation of AQP1. **a** Snapshot showing the single file of water molecules inside the channel. **b** Scheme of AQP1 showing the water dipole inversion (*green arrows*) during translocation through the channel. Adapted from de Groot and Grubmüller (2001), ISSN 0036-8075 (print), ISSN 1095-9203 (online). Reprinted with permission from AAAS

(Khandelia et al. 2009). A similar gating mechanism was proposed for AQPZ, an aquaporin that facilitates rapid water movements in *Escherichia coli*, where Arg^{189} (localised in loop D) flips between two possible positions that implicate different distances from Ala^{117}, which defines different conformations of the selectivity filter (Xin et al. 2011).

It was observed that water permeability coefficients for different members of the aquaporin family can be ordered according to the size of the pore (Hashido et al. 2005). These simulations indicate that the single water permeability coefficients present the following order:

$$\text{GlpF} \sim \text{AQPZ} > \text{AQP1} \gg \text{AQP0},$$

while their relative pore sizes can be ordered as follows:

$$\text{GlpF} \gg \text{AQP1} > \text{AQPZ} \gg \text{AQP0}.$$

According to the authors, these results (obtained using the TIP3P water model) may be explained taking into account the single-file nature presented by water molecules inside the pore. Nevertheless, other MD studies, using the same water model (TIP3P), reported that water flux and occupancy within carbon nanotubes can be reduced upon deformation of the pore (R. Wan et al. 2005). These results could indicate that distortion of the protein water channel could modify its water permeability coefficient. In the case of AQP1, experimental evidence suggests that a gating mechanism related to membrane tension could be possible (Fig. 5) (Ozu et al. 2011; Soveral et al. 2008; Wan et al. 2004).

AQP1 and AQP4 are the two members of the mammalian family that have been used in MD simulations to test their gating properties using the TIP4P water model (Hub et al. 2010). Recently, it was observed that the p_f of AQP1 and AQP4 depends on the electrostatic potential difference across the membrane. This relationship corresponds very well with a two-state model, i.e. open and closed states.

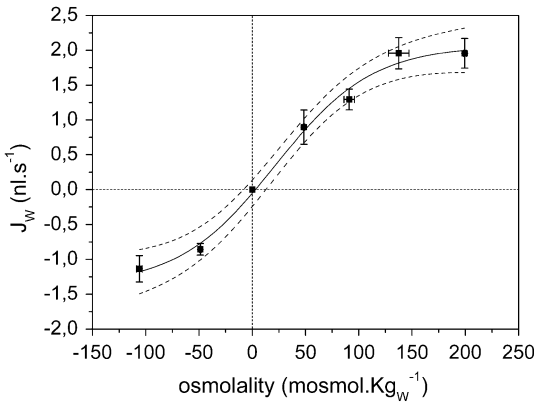

Fig. 5 Relationship between water flux (J_W) and osmolality measured in emptied-out oocytes expressing AQP1. According to theoretical bases (Finkelstein 1987) a linear relationship is expected. This result suggests a possible regulation of AQP1 dependent on membrane tension. With kind permission from Springer Science + Business Media: Ozu et al. (2011), figure 5

The results of this work predict a displacement of the Arg^{195} in AQP1 and the homolog Arg^{216} in AQP4, which are located at the selectivity filter, i.e. the ar/R region. In both cases, the open and closed states are defined by the distances between Arg^{195} and His^{180} in AQP1 and the homologues Arg^{216} and His^{201} in AQP4 (Hub et al. 2010). The predicted positions of the homologue arginine coincide with the two positions in which these residues were observed in the corresponding protein crystals (Ho et al. 2009; Sui et al. 2001). In addition, using the TIP3P water model it was observed that His^{201} is involved in a gating mechanism dependent on external electric fields and that the water dipole orientation in the selectivity filter is also affected (Garate et al. 2011).

Water models and aquaporins

Although different water models have been developed and validated through molecular dynamics, the models most widely employed by the scientific community are those quoted in Tables 1 and 2. Despite the apparent simplicity of these models, they are capable of reasonably reproducing many physical properties of water, both in conditions of bulk state and confinement state, and thus are adequate for use in studies that seek to characterise water behaviour in the neighbourhood of the plasma membrane as well as the intimacy of the aquaporin water channel.

Both the force field and the water model determine the behaviour of the system under study. In the framework of molecular dynamics of water within aquaporins, de Groot and Grubmüller (2001)—using SPC—as well as Jensen et al. (2003)—using TIP3P—concluded that proton translocation through AQPs is prevented by electrostatic barriers. However, Jensen et al. (2003), using the TIP3P model (CHARMM27 parameter set), observed very little disruption of the water-hydrogen-bonded network at the SF region of the AQPs pore, in contrast with the observation made by de Groot and Grubmüller (2001), using the SPC model (GROMACS force field). This differential behaviour could be attributed to force field differences (CHARMM vs. GROMACS) as well as the singularities of the different water models used.

The choice of a particular water model certainly influences the result obtained by the system under study, since different water models have different properties when simulated under exactly the same conditions. It has been shown that whilst SPC/E provides the best bulk water dynamics and structure, SPC gives less structure and faster diffusion, whereas TIP3P is characterised by even faster dynamics with a concomitantly greater structure loss when compared with the experimental values for liquid water (Mark and Nilsson 2001). Additionally, hydration thermodynamic properties of nonpolar and polar amino acid residues give different values depending on the water model employed. SPC/E shows hydration enthalpy and heat capacity of non-polar residues closer to the experimental values compared to SPC, TIP3P, TIP4P and TIP4P-Ew water models using the AMBER99, GROMOS 53A6 and OPLS-AA force fields (Hess and van der Vegt 2006). Additionally, complementary MD studies reported that different water models could lead to distinct structural arrangements of water inside a carbon nanotube. Namely, comparison between SPC/E and TIP3P models indicated that whilst the first model generates polygonal water structures inside the nanotube, the second one does not (Alexiadis and Kassinos 2008).

Since water-aquaporin interaction is the key factor in the behaviour of the system as a whole, a careful selection of the most adequate water model for each case study is mandatory. Consequently, a water model that presents a balanced overall ability to reproduce the actual behaviour of water should generally be the most reasonable option.

Nevertheless, a relevant property to give particular consideration for any chosen water model is the dielectric constant, given its most relevant role in every electrostatic interaction. If a model with a dielectric constant too far from the experimental value is chosen, the proper electrostatic interactions will most likely fail to manifest. On the other hand, if the protein-water interaction is case study optimised, modifying the rest of the force field parameters, this will result in changes in the electrostatic protein–protein interactions, which most likely will render an erroneous conformational behaviour of the macromolecule.

Likewise, a particularly important property for the study of water within aquaporins is the self-diffusion coefficient. Namely, it has been recently shown that this coefficient decreases in the presence of a hydrophobic membrane (Chara et al. 2009). Thus, the diffusional properties of water should expectedly be greatly influenced by such a high degree of confinement as that present within the aquaporin channel.

Based on the fact that the SPC/E model shows the most appropriately balanced overall compliance with the referred experimental properties (most of which are presented in Table 2), performing molecular dynamic studies of aquaporins using the SPC/E water model might render results of greater experimental accordance than those presently available in the literature.

So far, although comparison of the results obtained with SPC/E, against those produced using other models (Law and Samson 2004), points out the necessity of performing simulations of aquaporins with SPC/E, the use of this last model has been absent in the majority of the MD aquaporin studies (Table 4) up to date.

Enthusiastically, future water channel MD studies will become enhanced on account of a generalised increase in

Table 4 Water models used in MD simulations of nanopores, Gramicidin A and AQPs. Data in the table are chronologically ordered

Aquaporin	Water model	References
Gramicidin A	SPC	Chiu et al. (1989, 1991)
Nanopores	SPC/E	Lynden-Bell and Rasaiah (1996)
Nanopores	PSPC	Green and Lu (1997)
Gramicidin A	SPC/E	Chiu et al. (1999)
Nanopores	ST2	Allen et al. (1999)
Nanopores	SPC	Beckstein et al. (2001)
Nanopores	TIP3P	Hummer et al. (2001)
AQP1, GlpF	SPC	De Groot and Grubmüller (2001)
GlpF	TIP3P	Tajkhorshid et al. (2002)
Nanopores	SPC	Beckstein and Samson (2003)
GlpF	TIP3P	Jensen et al. (2003)
AQP1	SPC	de Groot et al. (2003)
Nanopores	SPC	Beckstein and Samson (2004)
Nanopores	TIP3P	Vaistheeswaran et al. (2004a, b)
AQP1	TIP3P	Zhu et al. (2004a, b)
GlpF	TIP3P	Chakrabarti et al. (2004)
Nanopores	TIP3P	Wan et al. (2005)
AQP0, AQP1, AQP4, AQPZ, GlpF	TIP3P	Hashido et al. (2005, 2007)
AQPZ, GlpF	TIP3P	Jensen and Mouritsen (2006)
AQP1	TIP4P	Hub and de Groot (2006, 2008)
Gramicidin A	TIP4P	Portella et al. (2007)
AQP1	TIP3P	Mamonov et al. (2007)
Nanopores	TIP3P	Gong et al. (2008)
AQP0	SPC	Jensen et al. (2008)
Gramicidin A	TIP4P	Portella and de Groot (2009)
SoPIP2;1	TIP3P	Khandelia et al. (2009)
AQP1, AQP4	TIP4P	Hub et al. (2010)
AQP1, AQP0	TIP3P	Qiu et al. (2010)
AQP4	TIP3P	Garate et al. (2011)
AQP1	TIP3P	Li et al. (2011)

At first sight it can be noticed that the first MD simulations used the SPC or the SPC/E water model in nanopores and Gramicidin A. Then, the works of Berezhkovskii and Hummer (2002), based on the methodology used by Hummer et al. (2001) and Zhu et al. (2004a) and Zhu et al. (2004b), settled the basics for MD in AQPs using the TIP3P water model; this has been the most frequently used since then

the consideration of the most appropriate water model to use when designing any state-of-the-art MD channel study. Finally, it is important to bear in mind that effective water models, such as those presently considered, are only surrogates to any model developed to consider the effects of both polarisation and quadrupole moment. Unhappily, such a water model still remains to be developed.

Concluding remarks

The dynamics of water in biological systems has been studied for many years. Although the discovery of aquaporins has allowed for the identification of the most relevant molecular entity responsible for water transport in biological systems, a profound understanding of water dynamics in these systems is far from complete. Moreover, several important controversies still persist.

Whilst most experimental approaches to study water transport at the cellular level are still based on the hydraulic characterisation of water pathways by means of macroscopic transport coefficients, molecular dynamics simulations provide, to some extent, a detailed mechanistic understanding of water at the molecular level. Whilst thermodynamics of irreversible processes form the theoretical framework behind the first hydraulic measurements, a mechanistic theory ruling osmotic phenomena at the molecular level in biological systems is still pending. Although such a theory does not yet exist, it can be stated that its elucidation most likely will involve the use of those models summarised in the previous sections. The challenge will be to understand the whole picture linking water transport inside aquaporins with their participation in/regulation by cellular and tissue processes under different physiological and patho-physiological scenarios. The years to come will reveal to what extent we will be able to address such a challenge.

Acknowledgments This work was financed by the Agencia Nacional de Promoción Científica y Tecnológica (ANCYPT) with the grant Prestamo BID PICT 2008 1564, awarded to OCH. MO is a Researcher from Universidad de Buenos Aires (UBA), HAA is a Ph.D. fellow of CONICET, ANMcC is a Career Research Member of CICPBA, and JRG and OCH are Career Research Members of CONICET.

References

Alexiadis A, Kassinos S (2008) Influence of water model and nanotube rigidity on the density of water in carbon nanotubes. Chem Eng Sci 63:2793–2797

Allen TW, Kuyucak S, Chung SH (1999) The effect of hydrophobic and hydrophilic channel walls on the structure and diffusion of water and ions. J Chem Phys 111(17):7985–7999

Báez LA, Clancy P (1994) Existence of a density maximum in extended simple point charge water. J Phys Chem 101(11): 9837–9840

Beckstein O, Samson MSP (2003) Liquid–vapor oscillations of water in hydrophobic nanopores. PNAS USA 100(12):7063–7068

Beckstein O, Samson MSP (2004) The influence of geometry, surface character, and flexibility on the permeation of ions and water through biological pores. Phys Biol 1(1–2):42–52

Beckstein O, Biggin PC, Samson MSP (2001) A hydrophobic gating mechanism for nanopores. J Phys Chem B 105(51):12902–12905

Beitz E, Wu B, Holm LM, Schultz JE, Zeuthen T (2006) Point mutations in the aromatic arginine region in aquaporin 1 allow passage of urea, glycerol, ammonia, and protons. PNAS USA 103(2):269–274

Bellati J, Alleva K, Soto G, Vitali V, Jozefkowicz C, Amodeo G (2010) Intracellular pH sensing is altered by plasma membrane PIP aquaporin co-expression. Plant Mol Biol 74(1–2):105–118

Berendsen HJC, Postma JPM, van Gunsteren WF, Hermans J (1981) Interaction models for water in relation to protein hydration. In: Pullman B (ed) Intermolecular forces. Reidel, Dordrecht

Berendsen HJC, Grigera JR, Straatsma TP (1987) The missing term in effective pair potentials. J Phys Chem 91(91):6269–6271

Berezhkovskii A, Hummer G (2002) Single-file transport of water molecules through a carbon nanotube. Phys Rev Lett 86(6):064503

Bernal JD, Fowler RH (1933) A theory of water and ionic solution, with particular reference to hydrogen and hydroxyl ions. J Chem Phys 1(8):515

Boehnke UC, Remmler T, Motschmann H, Wurlitzer S, Hauwede J, Fischer TM (1999) Partial air wetting on solvophobic surfaces in polar liquids. J Colloid Interface Sci 211(2):243–251

Burykin A, Warshel A (2003) What really prevents proton transport through aquaporin? Charge self-energy versus proton wire proposals. Biophys J 85(6):3696–3706

Burykin A, Warshel A (2004) On the origin of the electrostatic barrier for proton transport in aquaporin. FEBS Lett 570(1):41–46

Castner EW, Chang Y, Chu YC, Walrafen GE (1995) The intermolecular dynamics of liquid water. J Chem Phys 102(2):653–659

Chakrabarti N, Roux B, Pomès R (2004) Structural determinants of proton blockage in aquaporins. J Mol Biol 343:493–510

Chara O, McCarthy AN, Ferrara CG, Caffarena ER, Grigera JR (2009) Water behavior in the neighborhood of hydrophilic and hydrophobic membranes: lessons from molecular dynamics simulations. Phys A 388(21):4551–4559

Chara O, McCarthy AN, Grigera JR (2011) Crossover between tetrahedral and hexagonal structures in liquid water. Phys Lett A 375(3):572–576

Chau PL, Hardwick AJ (1998) A new order parameter for tetrahedral configurations. Mol Phys 93(3):511–518

Chiu SW, Subramaniam S, Jakobsson E, McCammon JA (1989) Water and polypeptide conformations in the gramicidin channel. A molecular dynamics study. Biophys J 56(2):253–261

Chiu SW, Jakobsson E, Subramahiam S, McCammon JA (1991) Time-correlation analysis of simulated water motion in flexible and rigid gramicidin channels. Biophys J 60(274):273–285

Chiu SW, Subramaniam S, Jakobsson E (1999) Simulation study of a gramicidin/lipid bilayer system in excess water and lipid I. Structure of the molecular complex. Biophys J 76(4):1929–1938

Cooper GJ, Zhou Y, Bouyer P, Grichtchenko II, Boron WF (2002) Transport of volatile solutes through AQP1. J Physiol 524(1): 17–29

Craig VSJ, Ninham BW, Pashley RM (1999) Direct measurement of hydrophobic forces: a study of dissolved gas, approach rate, and neutron irradiation. Langmuir 15(4):1562–1569

Danninger W, Zundel G (1981) Intense depolarized Rayleigh scattering in Raman spectra of acids caused by large proton polarizabilities of hydrogen bonds. J Chem Phys 74:2769–2777

de Groot BL, Grubmüller H (2001) Water permeation across biological membranes: mechanism and dynamics of aquaporin-1 and GlpF. Science 294(5550):2353–2357

de Groot BL, Frigato T, Helms V, Grubmüller H (2003) The mechanism of proton exclusion in the aquaporin-1 water channel. J Mol Biol 333(2):279–293

Deshmukh SA, Sankaranarayanan SKR (2012) Atomic scale characterization of interfacial water near an oxide surface using molecular dynamics simulations. Phys Chem Chem Phys 14:15593–15605

Ederth T, Liedberg B (2000) The influence of wetting properties on the long-range "hydrophobic" interaction between self-assembled alkylthiolate monolayers. Langmuir 16(5):2177–2184

Engel A, Fujiyoshi Y, Gonen T, Walz T (2008) Junction-forming aquaporins. Curr Opin Struct Biol 18(2):229–235

Errington JR, Debenedetti PG (2001) Relationship between structural order and the anomalies of liquid water. Nature 409(6818):318–321

Fang X, Yang B, Matthay MA, Verkman AS (2002) Evidence against aquaporin-1-dependent CO_2 permeability in lung and kidney. J Physiol 542(1):63–69

Fetter K, Van Wilder V, Moshelion M, Chaumont F (2004) Interactions between plasma membrane aquaporins modulate their water channel activity. Plant Cell 16:215–228

Finkelstein A (1987) Water movement through lipid bilayers, pores, and plasma membranes. Wiley, New York

Finkelstein A, Rosenberg P (1979) Single-file transport: implications for ion and water movement through gramicidin A channels. Membr Transp Process 3:77–88

Fischer G, Kosinska-Eriksson U, Aponte-Santamaría C, Palmgren M, Geijer C, Hedfalk K, Hohmann S, de Groot BL, Neutze R, Lindkvist-Petersson K (2009) Crystal structure of a yeast aquaporin at 1.15 angstrom reveals a novel gating mechanism. PLoS Biol 7(6):e1000130

Franks F (2000) Water: a matrix of life, 2nd edn. Royal Society of Chemistry, Cambridge, UK, p 225

Fu D, Libson A, Miercke LJ, Weitzman C, Nollert P, Krucinski J, Stroud RM (2000) Structure of a glycerol-conducting channel and the basis for its selectivity. Science 290(5491):481–486

Gale GM, Gallot G, Hache F, Lascoux N, Bratos S, Leicknam JC (1999) Femtosecond dynamics of hydrogen bonds in liquid water: a real time study. Phys Rev Lett 82(5):1068–1071

Garate JA, English NJ, MacElroy JMD (2011) Human aquaporin 4 gating dynamics in dc and ac electric fields: a molecular dynamics study. J Chem Phys 134(5):055110

Gentilcore AN, Michaud-Agrawal N, Crozier PS, Stevens MJ, Woolf TB (2010) Examining the origins of the hydration force between lipid bilayers using all-atom simulations. J Membr Biol 235:1–15

Giaya A, Thompson RW (2002) Water confined in cylindrical micropores. J Chem Phys 117(7):3464–3475

Gonen T, Silz P, Kistler J, Cheng Y, Walz T (2004) Aquaporin-0 membrane junctions reveal the structure of a closed water pore. Nature 429(6988):193–197

Gong X, Li J, Zhang H, Wan R, Lu H, Wang S, Fang H (2008) Enhancement of water permeation across a nanochannel by the structure outside the channel. Phys Rev Lett 101(25):257801

Gordillo MC, Nagy G, Marti J (2005) Structure of water nanoconfined between hydrophobic surfaces. J Chem Phys 123(5):054707

Graber DJ, Levy M, Kerr D, Wade WF (2008) Neuromyelitis optica pathogenesis and aquaporin 4. J Neuroinflammation 5:22

Green ME, Lu J (1997) Simulation of water in a small pore: effect of electric field and density. J Phys Chem B 101:6512–6524

Grigera JR, Kalko SG, Fischbarg J (1996) Wall-water interface. A molecular dynamics study. Langmuir 12(1):154–158

Gubskaya AV, Kusalik PG (2002) The total molecular dipole moment for liquid water. J Chem Phys 117(11):5290–5302

Guillot B (2002) A reappraisal of what we have learnt during three decades of computer simulations on water. J Mol Liq 101(1–3): 219–260

Han BG, Guliaev AB, Walian PJ, Jap BK (2006) Water transport in AQP0 aquaporin: molecular dynamics studies. J Mol Biol 360(2):285–296

Hashido M, Ikeguchi M, Kidera A (2005) Comparative simulations of aquaporin family: AQP1, AQPZ, AQP0 and GlpF. FEBS Lett 579(25):5549–5552

Hess B, van der Vegt NFA (2006) Hydration thermodynamic properties of amino acid analogs: a systematic comparison of biomolecular force fields and water models. J Phys Chem B 110:17616–17626

Hirano Y, Okimoto N, Kadohira I, Suematsu M, Yasuoka K, Yasui M (2010) Molecular mechanisms of how mercury inhibits water permeation through aquaporin-1: understanding by molecular dynamics simulation. Biophys J 98(8):1512–1519

Ho JD, Yeh R, Sandstrom A, Chorny I, Harries WEC, Robbins RA, Miercke LJW, Stroud RM (2009) Crystal structure of human aquaporin 4 at 1.8 Å and its mechanism of conductance. PNAS USA 106(18):7437–7442

Höchtl P, Boresch S, Bitomsky W, Steinhauser O (1998) Rationalization of the dielectric properties of common three-site water models in terms of their force field parameters. J Chem Phys 109(12):4927–4937

Horsefield R, Nordén K, Fellert M, Backmark A, Törnroth-Horsefield S, Terwisscha Van Scheltinga AC, Kvassman J, Kjellbom P, Johanson U, Neutze R (2008) High resolution x-ray structure of human aquaporin 5. PNAS USA 105(36):13327–13332

Hub JS, de Groot BL (2006) Does CO_2 permeate through Aquaporin-1? Biophys J 91(3):842–848

Hub JS, de Groot BL (2008) Mechanism of selectivity in aquaporins and aquaglyceroporins. PNAS USA 105(4):1198–1203

Hub JS, Aponte-Santamaría C, Grubmüller H, de Groot BL (2010) Voltage-regulated water flux through aquaporin channels in silico. Biophys J 99(12):L97–L99

Hummer G, Rasaiah JC, Noworyta JP (2001) Water conduction through the hydrophobic channel of a carbon nanotube. Nature 414:188–190

Ishibashi K, Hara S, Kondo S (2008) Aquaporin water channels in mammals. Clin Exp Nephrol 13(2):107–117

Israelachvili JN (1992) Intermolecular & surface forces, 2nd edn. Academic Press, San Diego

Israelachvili JN, McGuiggan PM (1988) Forces between surfaces in liquids. Science 241(4867):795–800

Israelachvili JN, Pashley R (1982) The hydrophobic interaction is long range, decaying exponentially with distance. Nature 300(5890):341–342

Jeffrey GA, Saenger W (1994) Hydrogen bonding in biological structures. Springer, New York

Jensen MØ, Mouritsen OG (2006) Single-channel water permeabilities of *Escherichia coli* aquaporins AqpZ and GlpF. Biophys J 90:2270–2284

Jensen MØ, Tajkhorshid E, Schulten K (2003) Electrostatic tuning of permeation and selectivity in aquaporin water channels. Biophys J 85(5):2884–2899

Jensen MØ, Dror RO, Xu H, Borhani DW, Arkin IT, Eastwood MP, Shaw DE (2008) Dynamic control of slow water transport by aquaporin 0: Implications for hydration and junction stability in the eye lens. Proceedings of the National Academy of Sciences USA 105(38):14430–14435

Jiang J, Daniels BV, Fu D (2006) Crystal structure of AqpZ tetramer reveals two distinct Arg-189 conformations associated with water permeation through the narrowest constriction of the water-conducting channel. J Biol Chem 281(1):454–460

Jorgensen WL, Madura JD (1985) Temperature and size dependence for Monte Carlo simulations of TIP4P water. Mol Phys 56(6):1381–1392

Jorgensen WL, Chandrasekhar J, Madura JD, Impey RW, Klein ML (1983) Comparison of simple potential functions for simulating liquid water. J Chem Phys 79(2):926–935

Jung JS, Preston GM, Smith BL, Guggino WB, Agre P (1994) Molecular structure of the water channel through aquaporin CHIP. The hourglass model. J Biol Chem 269(20):14648–14654

Kell GS (1975) Density, thermal expansivity, and compressibility of liquid water from 0° to 150°. Correlations and tables for atmospheric pressure and saturation reviewed and expressed on 1968 temperature scale. J Chem Eng Data 20(1):97–105

Khandelia H, Jensen MØ, Mouritsen OG (2009) To gate or not to gate: using molecular dynamics simulations to morph gated plant aquaporins into constitutively open conformations. J Phys Chem B 113(15):5239–5244

Kiselev M, Poxleitner M, Seitz-Beywl J, Heinzinger K (1993) An investigation of the structure of aqueous electrolyte solutions by statistical geometry. Z. Naturf A 48a:806–810

Krynicki K, Green CD, Sawyer DW (1978) Pressure and temperature dependence of self-diffusion in water. Faraday Discuss Chem Soc 66:199–208

Kumar P, Yan Z, Xu L, Mazza MG, Buldyrev SV, Chen SH, Sastry S, Stanley HE (2006) Glass transition in biomolecules and the liquid–liquid critical point of water. Phys Rev Lett 97(17):177802

Laenen R, Rauscher C, Laubereau A (1998) Dynamics of local substructures in water observed by ultrafast infrared hole burning. Phys Rev Lett 80(12):2622–2625

Law RJ, Samson MSP (2004) Homology modelling and molecular dynamics simulations: comparative studies of human aquaporin-1. Eur Biophys J 33(6):477–489

Lee SH, Rossky PJ (1994) A comparison of the structure and dynamics of liquid water at hydrophobic and hydrophilic surfaces: a molecular dynamics simulation study. J Chem Phys 100(4):3334–3345

Lee CY, McCammon JA, Rossky PJ (1984) The structure of liquid water at an extended hydrophobic surface. J Chem Phys 80(9):4448–4455

Lee JK, Kozono D, Remis J, Kitagawa Y, Agre P, Stroud RM (2005) Structural basis for conductance by the archaeal aquaporin AqpM at 1.68 Å. PNAS USA 102(52):18932–18937

Lerbret A, Lelong G, Mason PE, Saboungi ML, Brady JW (2011) Water confined in cylindrical pores: a molecular dynamics study. Food Biophys 6(2):233–240

Levitt DG (1973) Kinetics of diffusion and convection in 3.2-Å pores. Biophys J 13:186–206

Li H, Chen H, Steinbronn C, Wu B, Beitz E, Zeuthen T, Voth GA (2011) Enhancement of proton conductance by mutations of the selectivity filter of aquaporin-1. J Mol Biol 407(4):607–620

Lynden-Bell RM, Rasaiah JC (1996) Mobility and solvation of ions in channels. J Chem Phys 105(20):9266–9280

Mahoney MW, Jorgensen WL (2000) A five-site model for liquid water and the reproduction of the density anomaly by rigid, nonpolarizable potential functions. J Chem Phys 112(20): 8910–8922

Mahoney MW, Jorgensen WL (2001) Diffusion constant of the TIP5P model of liquid water. J Chem Phys 114(1):363–366

Mamonov AB, Coalson RD, Zeidel ML, Mathai JC (2007) Water and deuterium oxide permeability through aquaporin 1: MD predictions and experimental verification. J Gen Physiol 130(1): 111–116

Mark P, Nilsson L (2001) Structure and dynamics of the TIP3P, SPC and SPC/E water models at 298 K. J Phys Chem A 105: 9954–9960

Mathai JC, Agre P (1999) Hourglass pore-forming domains restrict aquaporin-1 tetramer assembly. Biochemistry 38(3):923–928

Modig K, Pfrommer BG, Halle B (2003) Temperature-dependent hydrogen-bond geometry in liquid water. Phys Rev Lett 90(7):075502

Möller C, Fotiadis D, Suda K, Engel A, Kessler M, Müller DJ (2003) Determining molecular forces that stabilize human aquaporin-1. J Struct Biol 142(3):369–378

Montrose CJ, Bucaro JA, Marshall-Coakley J, Litovitz TA (1974) Depolarized Rayleigh scattering and hydrogen bonding in liquid water. J Chem Phys 60(12):5025–5030

Mulders SM, Preston G, Deen P, Guggino W, Van Os C, Agre P (1995) Water channel properties of major intrinsic protein of lens. J Biol Chem 270(15):9010–9016

Murata K, Mitsuoka K, Hirai T, Walz T, Agre P, Heymann JB, Engel A, Fujiyoshi Y (2000) Structural determinants of water permeation through aquaporin-1. Nature 407(6804):599–605

Naberukhin YUI, Voloshin VP, Medvedev NN (1991) Geometrical analysis of the structure of simple liquids: percolation approach. Mol Phys 73(4):917–936

Nakhoul NL, Davis BA, Romero MF, Boron WF (1998) Effect of expressing the water channel aquaporin-1 on the CO_2 permeability of *Xenopus* oocytes. Am J Physiol Cell Physiol 274(2):C543–C548

Narten AH, Danford MD, Levy HA (1967) X-ray diffraction study of liquid water in the temperature range 4–200 °C. Discuss Faraday Soc 43:97–107

Neely JD, Christensen BM, Nielsen S, Agre P (1999) Heterotetrameric composition of aquaporin-4 water channels. Biochemistry 38(34):11156–11163

Neumann M (1986) Dielectric relaxation in water. Computer simulations with the TIP4P potential. J Chem Phys 85(3):1567–1580

Newby ZER, O'Connell J, Robles-Colmenares Y, Khademi S, Miercke LJ, Stroud RM (2008) Crystal structure of the aquaglyceroporin PfAQP from the malarial parasite *Plasmodium falciparum*. Nat Struct Mol Biol 15(6):619–625

Nienhuys HK, Woutersen S, van Santen RA, Bakker HJ (1999) Mechanism for vibrational relaxation in water investigated by femtosecond infrared spectroscopy. J Chem Phys 111(4):1494–1500

Ozu M, Dorr RA, Politi MT, Parisi M, Toriano R (2011) Water flux through human aquaporin 1: inhibition by intracellular furosemide and maximal response with high osmotic gradients. Eur Biophys J 40(6):737–746

Parisi M, Bourguet J (1983) The single file hypothesis and the water channels induced by antidiuretic hormone. J Membr Biol 71(3):189–193

Parisi M, Dorr RA, Ozu M, Toriano R (2007) From membrane pores to aquaporins: 50 years measuring water fluxes. J Biol Phys 33(5–6):331–343

Parker JL, Claesson PM (1994) Forces between hydrophobic silanated glass surfaces. Langmuir 10(3):635–639

Pimentel GC, McClellan AL (1960) The hydrogen bond. W. H. Freeman, San Francisco

Portella G, de Groot BL (2009) Determinants of water permeability through nanoscopic hydrophilic channels. Biophys J 96(3):925–938

Portella G, Pohl P, de Groot BL (2007) Invariance of single-file water mobility in gramicidin-like peptidic pores as function of pore length. Biophys J 92(11):3930–3937

Postma JPM (1985) MD of H_2O, a molecular dynamics study of water Thesis. University of Groningen

Prasad GVR, Coury LA, Finn F, Zeidel ML (1998) Reconstituted aquaporin 1 water channels transport CO_2 across membranes. J Biol Chem 273(50):33123–33126

Preston GM, Carroll TP, Guggino WB, Agre P (1992) Appearance of water channels in *Xenopus* oocytes expressing red cell CHIP28 protein. Science 256(5055):385–387

Preston GM, Jung JS, Guggino WB, Agre P (1993) The mercury-sensitive residue at cysteine 189 in the CHIP28 water channel. J Biol Chem 268(1):17–20

Qiu H, Ma S, Shen R, Guo W (2010) Dynamic and energetic mechanisms for the distinct permeation rate in AQP1 and AQP0. Biochim Biophys Acta 1798(3):318–326

Ren G, Cheng A, Reddy V, Melnyk P, Mitra AK (2000) Three-dimensional fold of the human AQP1 water channel determined at 4 Å resolution by electron crystallography of two-dimensional crystals embedded in ice. J Mol Biol 301:369–387

Saparov SM, Tsunoda SP, Pohl P (2005) Proton exclusion by an aquaglyceroprotein: a voltage clamp study. Biol Cell 97(7):545–550

Savage DF, Egea PF, Robles-Colmenares Y, O'Connell JD, Stroud RM (2003) Architecture and selectivity in aquaporins: 2.5 Å X-ray structure of aquaporin Z. PLoS Biol 1(3):E72

Schloerb PR, Friis-Hansen BJ, Edelman IS, Solomon AK, Moore FD (1950) The measurement of total body water in the human subject by deuterium oxide dilution. J Clin Investig 29(10):1296–1310

Sciortino F, Poole PH, Stanley HE, Havlin S (1990) Lifetime of the hydrogen bond network and gel-like anomalies in supercooled water. Phys Rev Lett 64(14):1686–1689

Sciortino F, Geiger A, Stanley HE (1991) Effect of defects on molecular mobility in liquid water. Nature 354:218–221

Shiratani E, Sasai M (1998) Molecular scale precursor of the liquid–liquid phase transition of water. J Chem Phys 108(8):3264–3276

Smith BL, Agre P (1991) Erythrocyte Mr 28,000 transmembrane protein exists as a multisubunit oligomer similar to channel proteins. J Biol Chem 266(10):6407–6415

Soper AK, Bruni F, Ricci MA (1997) Site–site pair correlation functions of water from 25 to 400 °C: revised analysis of new and old diffraction data. J Chem Phys 106(1):247–254

Soveral G, Madeira A, Loureiro-Dias MC, Moura TF (2008) Membrane tension regulates water transport in yeast. Biochim Biophys Acta 1778(11):2573–2579

Spohr E (1997) Molecular dynamics simulation studies of the density profiles of water between (9–3) Lennard-Jones walls. J Chem Phys 106(1):388–392

Steinhardt PJ, Nelson DR, Ronchetti M (1983) Bond-orientational order in liquids and glasses. Phys Rev B 28(2):784–805

Strauch HJ, Cummings PT (1989) Computer simulation of the dielectric properties of liquid water. Mol Simul 2(1–2):89–104

Striolo A, Chialvo AA, Cummings PT, Gubbins KE (2003) Water adsorption in carbon-slit nanopores. Langmuir 19(20):8583–8591

Striolo A, Gubbins KE, Chialvo AA, Cummings PT (2004) Simulated water adsorption isotherms in carbon nanopores. Mol Phys 102(3):243–251

Sui H, Han BG, Lee JK, Walian P, Jap BK (2001) Structural basis of water-specific transport through the AQP1 water channel. Nature 414:872–878

Tajkhorshid E, Nollert P, Jensen MØ, Miercke LJW, O'Connell J, Stroud RM, Schulten K (2002) Control of the selectivity of the aquaporin water channel family by global orientational tuning. Science 296(5567):525–530

Tani K, Mitsuma T, Hiroaki Y, Kamegawa A, Nishikawa K, Tanimura Y, Fujiyoshi Y (2009) Mechanism of aquaporin-4's fast and highly selective water conduction and proton exclusion. J Mol Biol 389(4):694–706

Törnroth-Horsefield S, Wang Y, Hedfalk K, Johanson U, Karlsson M, Tajkhorshid E, Neutze R, Kjellbom P (2006) Structural mechanism of plant aquaporin gating. Nature 439:688–694

Törnroth-Horsefield S, Hedfalk K, Fischer G, Lindkvist-Petersson K, Neutze R (2010) Structural insights into eukaryotic aquaporin regulation. FEBS Lett 584(12):2580–2588

Truskett TM, Torquato S, Debenedetti PG (2000) Towards a quantification of disorder in materials: distinguishing equilibrium and glassy sphere packings. Phys Rev E 62(1):993–1001

Tsao TH, Evans DF, Wennerstrom H (1993) Long-range attractive force between hydrophobic surfaces observed by atomic force microscopy. Science 262(5133):547–550

Vaistheeswaran S, Rasaiah JC, Hummer G (2004a) Electric field and temperature effects on water in the narrow nonpolar pores of carbon nanotubes. J Chem Phys 121(16):7955–7965

Vaistheeswaran S, Yin H, Rasaiah JC, Hummer G (2004b) Water clusters in nonpolar cavities. PNAS USA 101(49):17002–17005

van der Spoel D, van Maaren PJ, Berendsen HJC (1998) A systematic study of water models for molecular simulation: derivation of water models optimized for use with a reaction field. J Chem Phys 108(24):10220–10230

Vega C, Abascal JLF (2005) Relation between the melting temperature and the temperature of maximum density for the most common models of water. J Chem Phys 123(14):144504

Vega C, Sanz E, Abascal JLF (2005) The melting temperature of the most common models of water. J Chem Phys 122(11):114507

Verkman AS (2002) Does aquaporin-1 pass gas? An opposing view. J Physiol 524(1):31

Verkman AS, Mitra AK (2000) Structure and function of aquaporin water channels. Am J Physiol 278(1):F13–F28

Vidulich GA, Evans DF, Kay RL (1967) The dielectric constant of water and heavy water between 0 and 40.degree. J Phys Chem 71(3):656–662

Walz T, Smith BL, Zeidel ML, Engel A, Agre P (1994) Biologically active two-dimensional crystals of aquaporin CHIP. J Biol Chem 269(3):1583–1586

Wan X, Steudle E, Hartung W (2004) Gating of water channels (aquaporins) in cortical cells of young corn roots by mechanical stimuli (pressure pulses): effects of ABA and of $HgCl_2$. J Exp Bot 55(396):411–422

Wan R, Li J, Lu H, Fang H (2005) Controllable water channel gating of nanometer dimensions. JACS 127(19):7166–7170

Weng MH, Lee WJ, Ju SP, Chao CH, Hsieh NK, Chang JG, Chen HL (2008) Adsorption of water molecules inside a Au nanotube: a molecular dynamics study. J Chem Phys 128:174705

Woutersen S, Emmerichs U, Bakker HJ (1997) Femtosecond Mid-IR pump-probe spectroscopy of liquid water: evidence for a two-component structure. Science 278(5338):658–660

Wu Y, Tepper HL, Voth GA (2006) Flexible simple point-charge water model with improved liquid-state properties. J Chem Phys 124:024503

Xin L, Su H, Nielsen CH, Tang C, Torres J, Mu Y (2011) Water permeation dynamics of AqpZ: a tale of two states. Biochim Biophys Acta 1808:1581–1586

Yasui M, Hazama A, Kwon TH, Nielsen S, Guggino WB, Agre P (1999) Rapid gating and anion permeability of an intracellular aquaporin. Nature 402:184–187

Yeixeira J, Chen SH, Bellissent-Funel MC (1991) Molecular dynamics of liquid water probed by neutron scattering. J Mol Liq 48(2–4):111–121

Yu H, van Gunsteren WF (2004) Charge-on-spring polarizable water models revisited: from water clusters to liquid water to ice. J Chem Phys 121(19):9549–9564

Zampighi GA, Kreman M, Boorer KJ, Loo DD, Bezanilla F, Chandy G, Hall JE, Wright EM (1995) A method for determining the unitary functional capacity of cloned channels and transporters expressed in *Xenopus laevis* oocytes. J Membr Biol 148(1): 65–78

Zeidel ML, Ambudkar SV, Smith BL, Agre P (1992) Reconstitution of functional water channels in liposomes containing purified red cell CHIP28 protein. Biochemistry 31:7436–7440

Zhou X, Li CQ, Iwamoto M (2004) Equilibrium and kinetics: water confined in carbon nanotubes as one-dimensional lattice gas. J Chem Phys 121(16):7996–8002

Zhu SB, Robinson GW (1991) Structure and dynamics of liquid water between plates. J Chem Phys 94(2):1403–1410

Zhu F, Tajkhorshid E, Schulten K (2004a) Theory and simulation of water permeation in aquaporin-1. Biophys J 86(1):50–57

Zhu F, Tajkhorshid E, Schulten K (2004b) Collective diffusion model for water permeation through microscopic channels. Phys Rev Lett 93(22):224501